Chapter 2

Basic Concepts

2.1 Introduction

The intention of this chapter is to introduce the fundamental concepts of heterostructure laser diodes, waveguide analysis and threshold condition in semiconductor lasers. In section 2.2, the heterojunction and its properties are reviewed. In Section 2.3 Maxwell's equations is introduced. The applications of Maxwell's equations for slab waveguide analysis is demonstrated in section 2.4. In Section 2.5, the gain and loss considerations are discussed. Finally, the threshold condition is considered in section 2.6.

2.2 Heterostructure

Semiconductor heterojunctions (HJ's) or heterostructure are interfaces between dissimilar semiconductors, i.e. interfaces where the bandgap and/or electron affinity changes. The outstanding performance of many of today's optoelectronic devices is primarily due to the application of heterojunctions. These heterojunctions allow an optimized material combination in the device. They have strong influence on charge carriers and photons. They allow an easy exploitation of quantum-size effects [1].

In this section, the main properties of III-V heterojunctions are reviewed with reference to their application in optoelectronic devices. The different HJ types, as well as the most important material combinations, will briefly be described. Most attention

will be paid to semiconductor laser diodes in which a clever introduction of heterojunctions has led to very efficient and spectrally pure light sources.

2.2.1 Types of Heterojunctions

In many cases, the materials on both sides of a junction will be different in dopant density and/or type, like in a homojunction. Heterojunction in which the dopant type alters at the junction, is called anisotype (n-P or N-p, the capital letter indicating the larger bandgap side) junction. Junctions of the same dopant type are called isotype (n-N or p-P) junction. If the junction is sufficiently abrupt, the conduction and valence band will bend in such a way that a depletion or accumulation layer may arise. The formation of an accumulation layer on the lower-bandgap side of N^+-n^- or N^+-p^- HJ is the basic for the operation of the High Electron Mobility Transistor (HEMT). Whether the junction needs to be extremely abrupt (1 nm or less) or sligthly graded (e.g. 10 nm) depends on the application. For quantum wells or superlattices where the layers themselves are typically thinner than 10 nm, very abrupt transitions are required. In other applications, such as classical semiconductor laser or HBT's, the grading width may wider. The spike nature of an abrupt HJ may even be advantageous to the injection efficiency. No band bending will occur in a very slowly graded heterojunctionbut the charge carrier will undergo and additional force, different for electrons and holes, due to the conduction or valence band gradient. In equilibrium, this additional force will of course be compensated by diffusion forces. The abrupt to graded composition of compound semiconductor structures has led to the term "bandgap engineering". The extra design freedom offered

by heterojunctions is sometimes called the central design principle of heterostructure devices. Graded HJ's are sometimes applied in the base region of heterojunction bipolar transistor in order to decrease the electron transit time.

Heterojunctions can also be classified by their band line-up. Most practically used HJ's are of the stradding type (Fig. 2.1) also called "type I". These include GaAs-GaAlAs and InP-InGaAsP heterojunctions. Some III-V HJ's are the staggered or broken-gap type (call "type II").

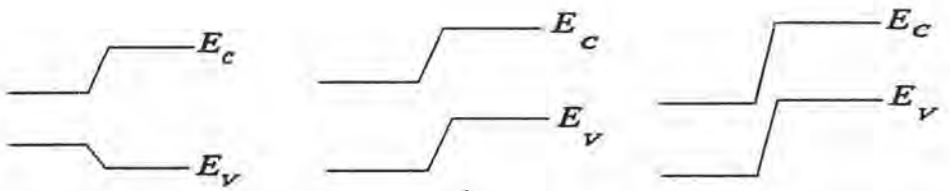

a) stradding b) staggered c) broken gap

Fig.2.1 Band line-up in heterojunctions

Following the Table 2.1, a further distinction can be made between lattice matchd and lattice mismatched junctions. In the case where low interface recombination velocities are required (e.g. laser diodes), a good lattice match is necessary. This can be illustrated by the following simplified expressions for the case of a double heterostructure (DH) lasers [2].

$$\eta = \frac{\frac{1}{\tau_r}}{\frac{1}{\tau_r} + \frac{1}{\tau_{nr}} + \frac{2S}{d}} \qquad (1)$$

Table 2.1 Types of Heterojunctions

Feature	Types
Dopant type	- Anisotype (N-p or P-n) - Isotype (N-n or P-p)
Interface width	- Abrupt - Graded in various degrees
Band line-up	- Type I stradding - Type II staggered or broken gap
Lattice constant	- Lattice Matched - Lattice mismatched
Polarity	- Polar on polar - Polar on non-polar
Band transition	- Direct on direct - Direct on indirect - Indirect on indirect
Interface structure	- Planar - Non-planar

Where η is the internal quantum efficiency, τ_r and τ_{nr} are the radiative and nonradiative minority lifetime, d is the active layer thickness and S is the interface recombination velocity, which follows an empirical relationship [2] ;

$$S \approx 2X10^{7}\ \Delta a/a_o \qquad cm/s \qquad (2)$$

in which $\Delta a/a_o$ is the relative lattice mismatch. From these expressions it is clear that very low $\Delta a/a_o$ value (typically$<10^{-4}$) is necessary, especially for very thin active layers.

In a number of cases, lattice mismatch is introduced on purpose or from necessity. When the lattice constant of the entire device structure is different from the substrate material, care will be taken to avoid high defect concentration in the device. GaAsP homojunction LED's, for example a slowly graded GaAsP layer, several tens of microns thick, will be grown as a buffer layer between the substrate (GaAs if $X_{As}>0.5$ or GaP if $X_{As}<0.5$) and the device layers. Although the final layer still has a relatively high dislocation density, relatively large area and low integration-density LED's can be produced with very high internal efficiency. A more recent development is the growth of GaAs on Si, with obvious applications in solar cell, laser diodes, and in the integration of Si circuits with light emitters. This heterojunction is not only hindered by the 4% mismatch but also, and perhaps more important, by the transition from a non-polar semiconductor, which can easily lead to antiphase disorder. Lattice mismatch is introduced on purpose in strained layer superlattice (SLS). In these periodic layer structures, the mismatch is accommodated by elastic forces. As long as the layer thickness is below a certain critical value, no misfit dislocations

appear in these layers. SLS's find several applications in optoelectronics because of their flexibility in material combination and because of the increase bandgap with compression and tension. Other classifications can also be made. In optoelectronic devices, the band transition (whether direct or indirect) is important. At the HJ, the predominant conduction band may be different on each side, leading to an influence on the charge transport across the junction.

A heterojunction may be formed by growth on a non-planar substrate or layer. Although such a non-planar HJ may not have distinct properties compared with a planar one, this class of HJ's deserves being mentioned because it is often making laser diodes and, in addition, various epitaxial growth processes behave quite different from to non-planar growth.

2.2.2 Advantages of Using HJ's

The advantages of using heterojunctions have already been indicated in the introduction. It is interesting to see that many of these advantages had been predicted long before the fabrication technology provide experimental verification. The useful properties of HJ's can be divided into four main categories. These will be discussed briefly.

A. Combination of different semiconductors in the same device

The use of HJ's does indeed allow for different materials in different places of device. The junction, i.e. the interface, itself

is not of prime importance here and should behave properly.

A typical case is when a certain compound is not suited for contact (either Ohmic or Schottky). Another III-V compound are then grown on the top of the original material. In GaAs-GaAlAs laser diodes, for example, a GaAs layer is always used on the top of the AlGaAs cladding layers in order to facilitate ohmic contacting (which in general is always easier on the lower bandgap materials). In InGaAs MESFETs the low Schottky barrier height creates a problem. The application of a GaAs overlayer (though mismatched) for making Schottky contact has been proposed [3].

Another example is the mainly of optoelectronic devices where a transparent layer (high bandgap) is used as an interface between the device and air. Besides, consideration of electrical or thermal conductivity or carrier lifetime sometimes motivates a change of material in order to enhance the overall properties.

B. Impact on Charge Carriers

The impact of HJ's on charge carriers is twofold. First, a very high injection efficiency is obtained in an anisotype HJ for carriers from high bandgap side. This injection efficiency is related to the charge in the bandgap in an exponential way. It means that the injection efficiency can be made virtually independent of doping levels. In heterojunction LED's, for example, this property implies that the doping levels can be optimized for maximum internal radiative efficiency.

The second advantage is the confinement of minority carriers. An HJ is indeed able to form a barrier to the flow of minority carriers to the higher bandgap side. In this way, a steep concentration efficiency for electrons or holes is particularly related to the conduction or valence band discontinuity but is often further enhanced by the electric field in the depletion layer. Even if the bandgap charge is taken up entirely by a valence band discontinuity, probably as in a GaAs-InGaP HJ electron confinement, can be obtained by proper doping levels on each side of the junction.

In double heterostructure, as normally used in laser diode, the injection efficiency and carrier confinement work together to obtain high carrier concentrations in active layer (possibly higher than the doping densities in the injecting layers). The thinner active layer, the higher carrier concentration is required for a given current, since optical gain (stimulated recombination) increase with carrier density. The application of a double heterostructure (DH) is essential to obtain a low threshold laser diode.

C. Impact on Photons

An HJ,in general, inherits a step in refractive index. Most III-V compounds have refractive indices between 3 and 4. Although not a rule, the refractive index and bandgap do change in opposite directions with change in composition for many ternary and quaternary compounds. Through this property, the DH structure confines not only charge carriers but also photons by total internal reflection. DH's behave as optical waveguides.

The thickness of the DH waveguide as used in the laser diode is important in two ways. Firstly, it defines the optical confinement Γ of the travelling mode, i.e. the percentage of optical power being confined in the layer. If Γ is low, most power will travel in the lossy layer, which is of course an undesireable. Secondly, the beam divergence angle θ, preferably low, strongly depends on the active layer thickness. Both Γ, θ and optical gain g in the active layer are shown as a function of layer thickness d in fig.2.2. Very thin layers have high gain but low Γ, whereas the opposite is true for thick layers. Clearly, an optimal exists in between, typically at a layer thickness of 0.1 μm. At this value, θ is normally decreasing with decreasing layer thickness.

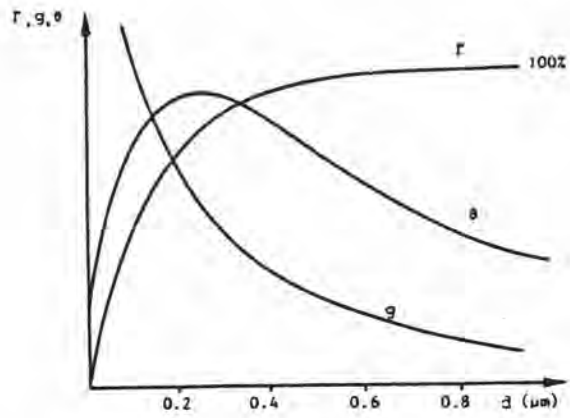

Fig.2.2 Optical confinement Γ, emission angle θ and gain g of DH lasers as function of active layer thickness.

The index change at an HJ can also be used for reflection at normal incidence. Although the index change is relatively small, and the reflection on one interface, therefore, is very small, subsequent layers may show high reflection by constructive

interference. This is the case in the so-called Bragg reflector, consisting of the stack of periodic layers with alternate compositions and quarter wavelength thicknesses. The reflectivity of a 20-period GaAs-AlGaAs reflector, as seen from air, is shown in Fig.2.3 as a function of Al content. Very high reflection coefficients can be obtained in this way. Bragg reflectors are very promosing for applications in surface emitting lasers.

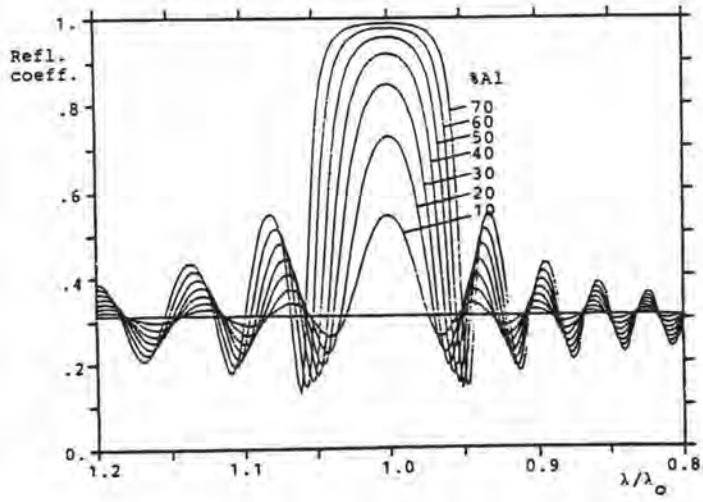

Fig.2.3 Reflection from 20-period GaAs-GaAlAs Bragg reflector [1].

D. Quantum wells and Superlattices

Current epitaxial growth techniques can form very thin abrupt HJ interfaces. In this way, it is possible to realize potential wells whose dimensions areof the order of the de Broglie wavelength and of the mean free path of the free charge particles. Quantization of confined particle states may then occur. Periodic extensions of thin layer pairs, superlattices, imposes an artificial periodicity on the crystal structure and exhibit new properties.

The potential of the application of quantum wells and superlattices for optoelectronic devices is not all that clear. Their application in semiconductor lasers has various effects as discussed in the next paragraph, the most important being the wavelength shift [4]. The application in avalanche photodetectors has been mentioned before. Superlattices show strong optical nonlinearities in both the reflective index and the absorption [5], especially close to the absorption edge. This has stimulated much research in all-optical switches for optical logic, but as of now it seems that these devices are still very far away from practical use. Quantum well structures are also interesting for high speed operation of devices. Very short pulses have been obtained from laser diodes by mode-locking with quantum well saturable absorber [6]. High speed optical modulator has been demonstrated by exploited the quantum-confinement stack effect [7].

2.3 Maxwell's equations

Maxwell's equations, the basis of electromagnetic field theory, are the relationship between the electric charge density, ρ, electric field, E, electric displacement, D, magnetic field, H, and magnetic induction, B. An auxiliary equation the continuity equation relates the current and charge sources [8], [9].

Maxwell's equations are important to this work because the solution or a certain set conditions leads to the mathematical description of the plane wave with the sinusoidal variation in time and position of E and H with the amplitude of each being constant in the plane normal to the direction of propagation.

In differential form, Maxwell's equations are

$$\frac{\delta E^2}{\delta X^2} + [K_o^2 n_o^2 - \beta^2] E = 0 \qquad (3\text{-a})$$

and

$$\frac{\delta H^2}{\delta Y^2} + [K_o^2 n_o^2 - \beta^2] H = 0 \qquad (3\text{-b})$$

Boundary condition

A planar interface is an abrupt boundary at which properties change discontinously, e.g. at an air-material boundary. Firstly, we consider the electric displacement for the pill box in Fig.2.4. If there is no free surface charge at the boundary, then as the width of the no charge in the pill box appoaches zero.

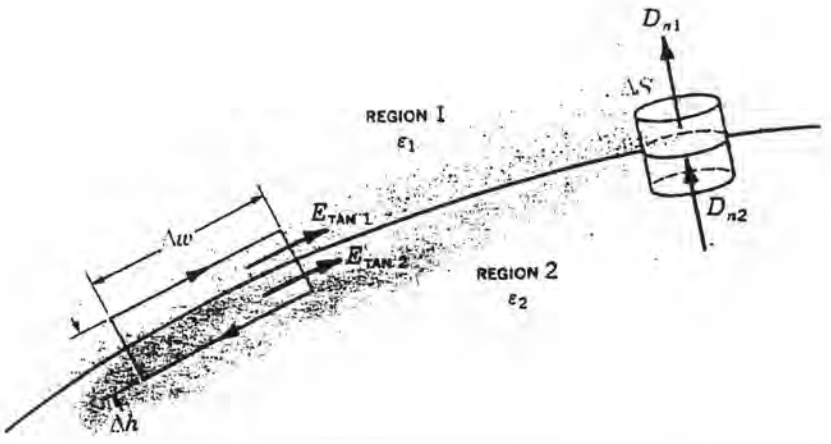

Fig.2.4 Geometry for computation of the boundary conditions

Thus, the normal component of D is continous across a boundary containing no free charge

$$D_{n1} = D_{n2} \tag{4}$$

as the distance normal to the interface and, therefore, the area of the loop appoaches zero. Thus

For the electric field in Fig.2.4

$$E_{t1} = E_{t2} \tag{5}$$

across an interface where E_t is the tangential component of E. Using similar arguments, one can show that

$$B_{n1} = B_{n2} \tag{6}$$

where B_n is the normal component of the magnetic induction vector. Also,

$$H_{t1} = H_{t2} \tag{7}$$

where H_t is the tangential component of the magnetic field.

2.4 Waveguide Analysis

In this section, the waveguide properties are analyzed based on the effective index approximation. Only TE mode is considered in the calculation because of the superiority to TM mode in the structure. The electric field distribution and the eigen-value equation for each structure are derived from Maxwell's equation.

2.4.1 Three-Layer Slab Waveguide (DH Structure)

The structure of three-layer slab waveguide is shown in Fig.2.5.

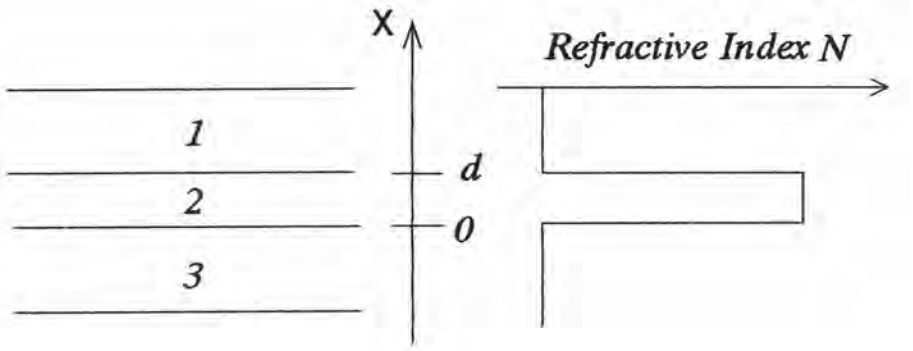

Fig.2.5 The schematic diagram of three-layer slab waveguide where $N_1 = N_3 < N_2$.

The field distribution of three-layers slab waveguide is [10]

$$E(x) = A_1 \exp(r_1 x) \qquad x<0 \qquad (8)$$

$$= A_2 \cos(h_2 x) + A_3 \sin(h_2 x) \qquad 0<x<d \qquad (9)$$

$$= A_4 \exp(-r_3 (x-d)) \qquad d<x \qquad (10)$$

where A_1, A_2, A_3 and A_4 are arbitrary constants

$$K_o = 2\pi/\lambda \qquad (11\text{-a})$$

$$r_1 = K_o \sqrt{N_{eff}^2 - N_1^2} \qquad (11\text{-b})$$

$$h_2 = K_o \sqrt{N_2^2 - N_{eff}^2} \qquad (11\text{-c})$$

$$r_3 = K_o \sqrt{N_{eff}^2 - N_3^2} \qquad (11\text{-d})$$

The relation of arbitrary constants are shown in equation (12), (13) and (14)

$$A_2 = A_1 \tag{12}$$

$$A_3 = (r_1/h_2)A_1 \tag{13}$$

$$A_4 = (\cos(h_2 d)+(r_1/h_2)\sin(h_2 d))A_1 \tag{14}$$

The eigen value equation of this problem is given as follows:

$$\mathrm{TAN}(h_2 d) = \frac{h_2(r_1+r_3)}{(h_2^2-r_1 r_3)} \tag{15}$$

The example of the numerical evaluation of the effective refractive index of this structure is shown in Fig. 2.6

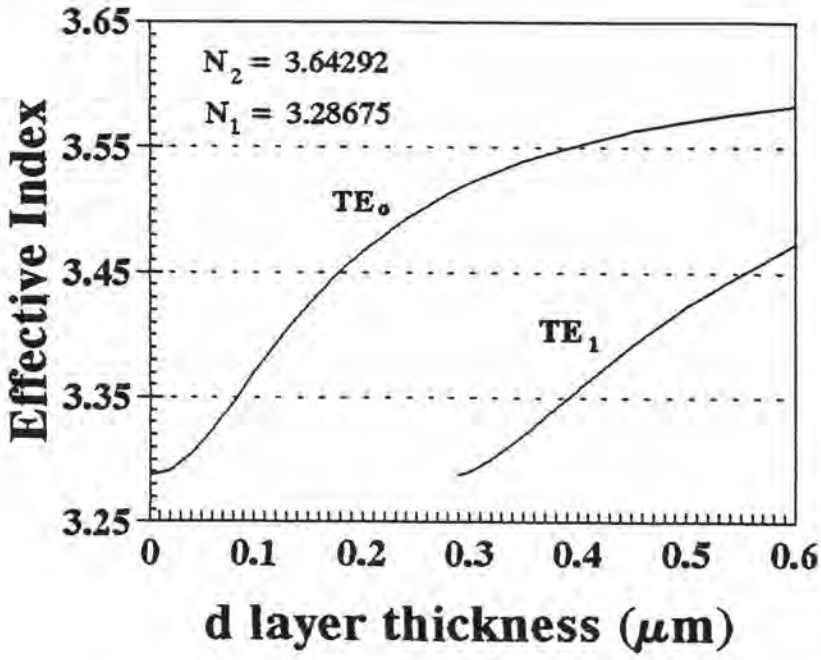

Fig.2.6 Effective index of symmetric three-layer slab waveguide.

2.4.2 Four-Layer Slab Waveguide (Four-Layer Heterostructure)

The structure of four-layer slab waveguide is shown in Fig.2.7.

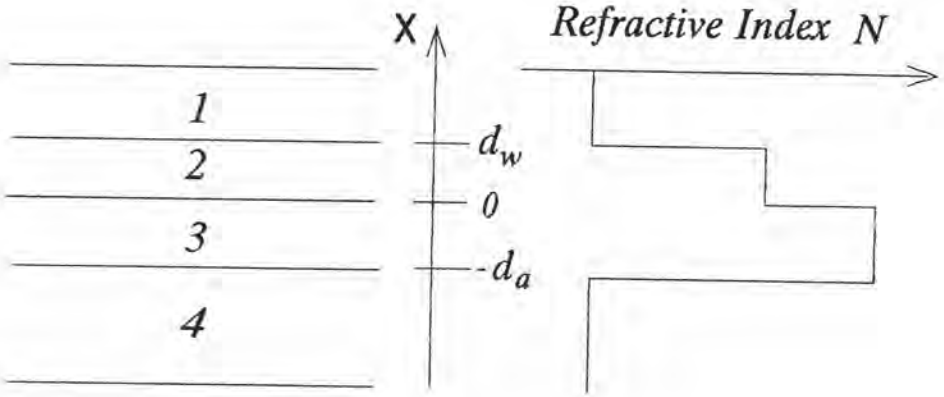

Fig.2.7 The schematic diagram of four-layer slab dielectric waveguide where $N_1 = N_4 < N_2 < N_3$.

The field distribution of four-layer slab waveguide is [11]

$$E(x) = A_1 \exp(-r_1(x-d_w)) \qquad d_w < x \qquad (16)$$

$$= A_2\cos(h_2x)+A_3\sin(h_2x) \qquad 0<x<d_w \qquad (17)$$

$$= A_4\cos(h_3x)+A_5\sin(h_3x) \qquad -d_a<x<0 \qquad (18)$$

$$= A_6.\exp(r_4.(x+d_a)) \qquad x<-d_a \qquad (19)$$

where A_1, A_2, A_3 and A_4 are arbritrary constants

$$K_o = 2\pi/\lambda \qquad (20\text{-a})$$

$$r_1 = K_o\sqrt{N_{eff}^2-N_1^2} \qquad (20\text{-b})$$

$$h_2 = K_o\sqrt{N_2^2-N_{eff}^2} \qquad (20\text{-c})$$

$$h_3 = K_o\sqrt{N_3^2-N_{eff}^2} \qquad (20\text{-d})$$

$$r_4 = K_o\sqrt{N_{eff}^2-N_4^2} \qquad (20\text{-e})$$

The relations of arbitrary constants are given by equation (21), (22), (23), (24) and (25)

$$A_2 = A_1[\cos(h_2 d_w)+(r_1/h_2)\sin(h_2 d_w)] \quad (21)$$

$$A_3 = A_1[\sin(h_2 d_w)-(r_1/h_2)\cos(h_2 d_w)] \quad (22)$$

$$A_4 = A_2 \quad (23)$$

$$A_5 = (h_2/h_3)A_3 \quad (24)$$

$$A_6 = A_4\cos(h_3 d_a)-A_5\sin(h_3 d_a) \quad (25)$$

The eigen-value equation of this problem is given as follows:

$$\mathrm{TAN}(h_3 d_w) = \frac{A_4 r_4 - A_5 h_3}{A_5 r_4 - A_4 h_3} \quad (26)$$

The example of the numerical evaluation of the effective refractive index of this structure is shown in Fig.2.8

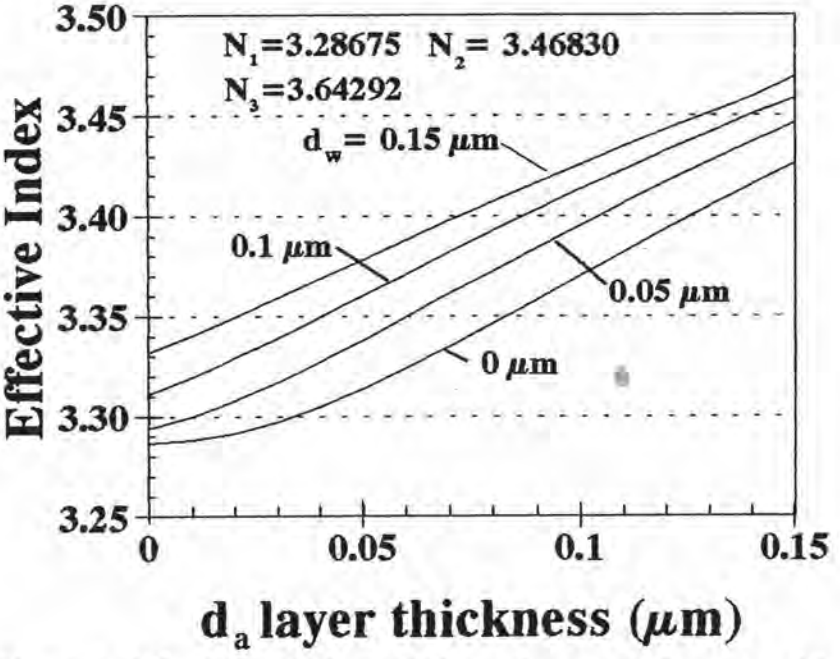

Fig.2.8 Effective index of four-layer slab waveguide.

2.4.3 Five-Layer Slab Waveguide (SCH Structure)

The structure of five-layer slab waveguide is shown in Fig.2.9.

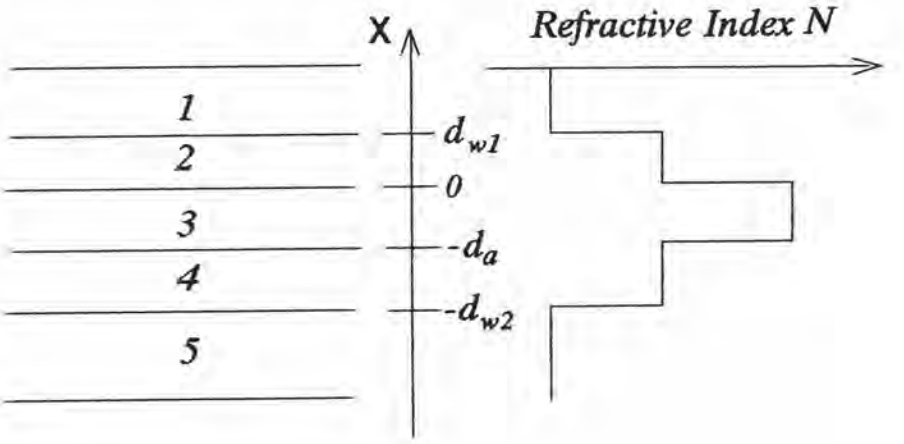

Fig.2.9 The schematic diagram of five-layer slab dielectric waveguide where $N_1=N_5 < N_4=N_2 < N_3$.

The field distribution of five-layer slab waveguide is [12]

$$E(x) = A_1\exp(-r_1(x-d_{w1})) \qquad d_{w1}<x \qquad (27)$$

$$= A_2\cos(h_2x)+A_3\sin(h_2x) \qquad 0<x<-d_{w1} \qquad (28)$$

$$= A_4\cos(h_3x)+A_5\sin(h_3x) \qquad -d_a<x<0 \qquad (29)$$

$$= A_6\cos(h_4(x+d_a))+A_7\sin(h_4(x+d_a)) \qquad -(d_a+d_{w2})<x<-d_a \qquad (30)$$

$$= A_8\exp(r_5(x+(d_a+d_{w2})) \qquad x<-(d_a+d_{w2}) \qquad (31)$$

where A_1, A_2, A_3, A_4, A_5, A_6, A_7 and A_8 are arbitrary constants.

$$K_o = 2\pi/\lambda \qquad (32\text{-a})$$

$$r_1 = K_o\sqrt{N_{eff}^2-N_1^2} \qquad (32\text{-b})$$

$$h_2 = K_o\sqrt{N_2^2-N_{eff}^2} \qquad (32\text{-c})$$

$$h_3 = K_o\sqrt{N_3^2-N_{eff}^2} \qquad (32\text{-d})$$

$$h_4 = K_o\sqrt{N_4^2-N_{eff}^2} \qquad (32\text{-}e)$$

$$r_5 = K_o\sqrt{N_{eff}^2-N_5^2} \qquad (32\text{-}f)$$

The relations of arbitrary constants are given by equation (33), (34), (35), (36), (37), (38) and (39)

$$A_2 = A_1[\cos(h_2 d_{w1})+(r_1/h_2)\sin(h_2 d_{w1})] \qquad (33)$$

$$A_3 = A_1[\sin(h_2 d_{w1})-(r_1/h_2)\cos(h_2 d_{w1}))] \qquad (34)$$

$$A_4 = A_2 \qquad (35)$$

$$A_5 = (h_2/h_3)A_3 \qquad (36)$$

$$A_6 = A_4\cos(h_3 d_a)-A5\sin(h_2 d_a) \qquad (37)$$

$$A_7 = (h_3/h_4)[A_4\sin(h_3 d_a)+A_5\cos(h_3 d_a)] \qquad (38)$$

$$A_8 = [A_6\sin(h_4 d_{w2})+A_7\cos(h_4 d_{w2})] \qquad (39)$$

The eigen-value equation of this problem is griven as follows:

$$TAN(h_4 d_{W2}) = \frac{-(h_4 A_7+r_5 A_4)}{(r_6 A_7-h\ A_4)} \qquad (40)$$

The example of the numerical evaluation of the effective refractive index of this structure is shown in Fig.2.10.

$$h_4 = K_o\sqrt{N_4^2-N_{eff}^2} \qquad (32\text{-e})$$

$$r_5 = K_o\sqrt{N_{eff}^2-N_5^2} \qquad (32\text{-f})$$

The relations of arbitrary constants are given by equation (33), (34), (35), (36), (37), (38) and (39)

$$A_2 = A_1[\cos(h_2 d_{w1})+(r_1/h_2)\sin(h_2 d_{w1})] \qquad (33)$$

$$A_3 = A_1[\sin(h_2 d_{w1})-(r_1/h_2)\cos(h_2 d_{w1}))] \qquad (34)$$

$$A_4 = A_2 \qquad (35)$$

$$A_5 = (h_2/h_3)A_3 \qquad (36)$$

$$A_6 = A_4\cos(h_3 d_a)-A5\sin(h_2 d_a) \qquad (37)$$

$$A_7 = (h_3/h_4)[A_4\sin(h_3 d_a)+A_5\cos(h_3 d_a)] \qquad (38)$$

$$A_8 = [A_6\sin(h_4 d_{w2})+A_7\cos(h_4 d_{w2})] \qquad (39)$$

The eigen-value equation of this problem is griven as follows:

$$TAN(h_4 d_{W2}) = \frac{-(h_4 A_7+r_5 A_4)}{(r_5 A_7-h\ A_4)} \qquad (40)$$

The example of the numerical evaluation of the effective refractive index of this structure is shown in Fig.2.10.

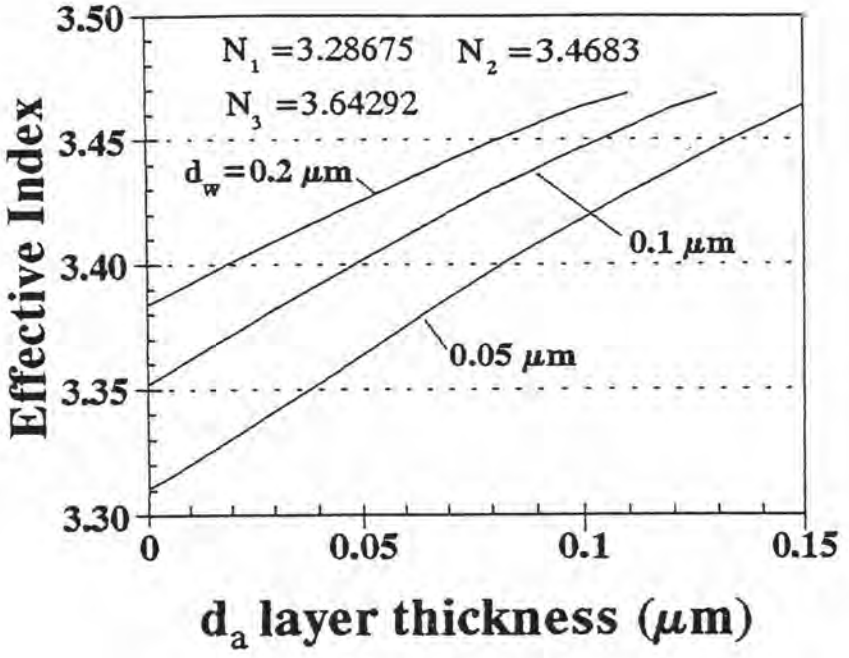

Fig.2.10 Effective index of symmetric five layers slab waveguide.

Table 2.2 Refractive indices of GaAs and GaAlAs at 0.88 μm [13].

Al Content (%) in GaAlAs	Refractive Index
GaAs (X_{Al}=0)	3.64292
GaAlAs (X_{Al}=20%)	3.46830
GaAlAs (X_{Al}=30%)	3.40623
GaAlAs (X_{Al}=50%)	3.28675
GaAlAs (X_{Al}=60%)	3.22779

2.4.4 Confinement Factor

Confinement factor is defined as the ratio of the light intensity within the active layer to the sum of the light intensity both within and outside the active layer [14]. Using E(x) of DH structure from equations (8)-(10), Γ for DH structure is given by equation (38) and an example of calculation for GaAs-GaAlAs DH structure is shown in Fig.2.11.

$$\Gamma = \frac{\int_{0}^{d} E(X)dX}{\int_{-\infty}^{\infty} E(X)dX} \qquad (41)$$

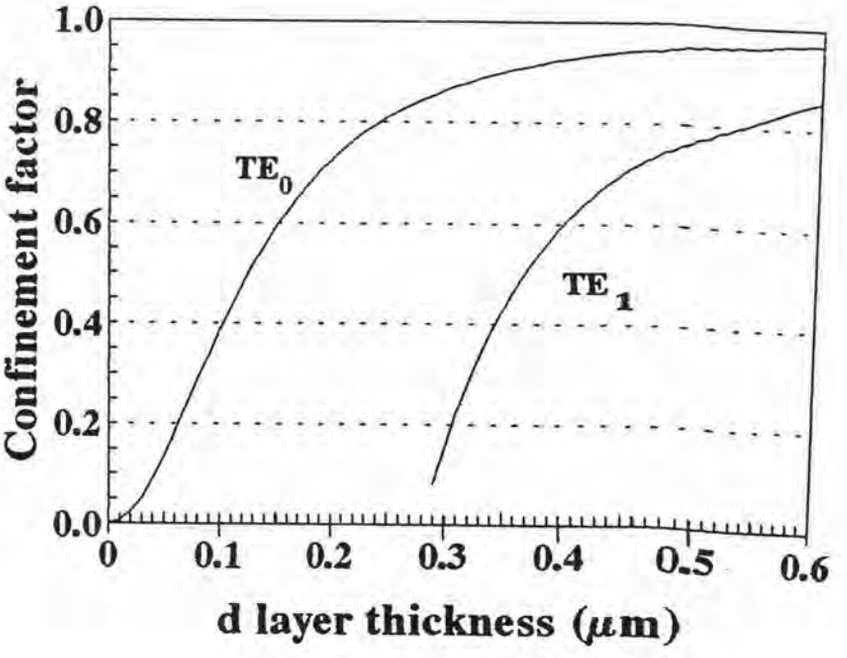

Fig.2.11 Confinement factor for GaAs-GaAlAs (X_{Al}=0.5) DH structure as a function of active layer thickness.

2.5 Threshold condition

In this section, the basics of linear gain theory, the threshold condition and threshold current density of semiconductor material are reviewed.

2.5.1. Linear Gain Theory

Theory of linear gain is one of the most basic properties of semiconductor. The peak gain can be approximated by [15], [16]

$$\alpha_p = A_o(n-N_g) \qquad (42)$$

where A_o is the gradient of α_p versus n, the injected carrier concentration, N_g is the injected carrier density at which the peak gain is equal to zero

The gain parameters of equation (39) are approximated as

$$A_o = 3.2\text{x}10^{-16}\exp(-E_g/3.4) \quad \text{cm}^2 \qquad (43)$$

$$N_g = 5.0\text{x}10^{17}.\exp(E_g/0.96) \quad \text{cm}^{-3} \qquad (44)$$

At 300 K, the E_g of GaAs is 1.424 eV. By using equations (43) and (44), A_o is $2.105\text{X}10^{-16}$ cm^2 and N_g is $2.204\text{X}10^{18}$ cm^{-3}.

2.5.2 Theshold Current Density

The threshold condition in laser is that the mode gain (G_m) is equal to the loss (A) in the optical cavity. The mode gain is

2.5 Threshold condition

In this section, the basics of linear gain theory, the threshold condition and threshold current density of semiconductor material are reviewed.

2.5.1. Linear Gain Theory

Theory of linear gain is one of the most basic properties of semiconductor. The peak gain can be approximated by [15], [16]

$$\alpha_p = A_o(n-N_g) \qquad (42)$$

where A_o is the gradient of α_p versus n, the injected carrier concentration, N_g is the injected carrier density at which the peak gain is equal to zero

The gain parameters of equation (39) are approximated as

$$A_o = 3.2\text{x}10^{-16}\exp(-E_g/3.4) \quad \text{cm}^2 \qquad (43)$$

$$N_g = 5.0\text{x}10^{17}.\exp(E_g/0.96) \quad \text{cm}^{-3} \qquad (44)$$

At 300 K, the E_g of GaAs is 1.424 eV. By using equations (43) and (44), A_o is $2.105\text{X}10^{-16}$ cm^2 and N_g is $2.204\text{X}10^{18}$ cm^{-3}.

2.5.2 Theshold Current Density

The threshold condition in laser is that the mode gain (G_m) is equal to the loss (A) in the optical cavity. The mode gain is

given by

$$G_m = \Gamma g \tag{45}$$

where g is the local gain, and Γ is the optical confinement factor in the active layer. The gain in the active layer of the semiconductor laser depends on the loss in the laser as follows :

$$A = (1/2L)\ln((1/R_1R_2)+\alpha_{ex}(1-\Gamma)+\alpha_{in}\Gamma \tag{46}$$

Where α_{ex} is external modal loss, α_{in} is the internal modal loss in active layer, R_1 and R_2 are the front facet and rear facet modal reflectivities and L is the cavity length.

At threshold, the gain peak of the linear gain in the active region is equal to the total loss in the laser

$$A = g\Gamma \tag{47}$$

Using equation (39) and (44), the carrier concentration in active layer at threshold

$$n_{th} = (A/A_o\Gamma+N_g) \tag{48}$$

A determination of the threshold current density depends on the carrier concentration in active layer at threshold condition [17] as

$$J_{th} = qdB_o n_{th}^2 \tag{49}$$

where q is the electronic charge, B_o is the band-to-band recombination coefficient for the GaAs, $B_o = 1X10^{-10}$ cm^{-3}/second [18] and d is the active layer thickness.